Removal of nutrients from pulp and paper biorefinery effluent: operation, kinetic modelling and optimization by response surface methodology

Ahmad Hussaini Jagaba[1,2*], Shamsul Rahman Mohamed Kutty[1], Mu. Naushad[3], Ibrahim Mohammed Lawal[4], Azmatullah Noor[1], Augustine Chioma Affam[5,6], Abdullahi Haruna Birniwa[7], Sule Abubakar[2], Usman Bala Soja[8], Kunmi Joshua Abioye[9], Chinna Bathula[10]

[1]Department of Civil and Environmental Engineering, Universiti Teknologi PETRONAS, Bandar Seri Iskandar 32610, Perak Darul Ridzuan, Malaysia

[2]Department of Civil Engineering, Abubakar Tafawa Balewa University, Bauchi, Nigeria

[3]Department of Chemistry, College of Science, King Saud University, P.O. Box 2455, Riyadh 11451, Saudi Arabia

[4]Department of Civil and Environmental Engineering, University of Strathclyde, Glasgow, UK.

[5]Civil Engineering Department, School of Engineering and Technology, University of Technology Sarawak, Persiaran Brooke, 96000 Sibu, Sarawak, Malaysia

[6]Centre of Research for Innovation and Sustainable Development (CRISD), University of Technology Sarawak, Sibu, Malaysia

[7]Department of Chemistry, Sule Lamido University, PMB 048 Kafin-Hausa, Nigeria

[8]Department of Civil Engineering, Federal University Dutsin-Ma, Dutsin-Ma P.M.B. 5001, Katsina State, Nigeria

[9]Department of Chemical Engineering, Universiti Teknologi PETRONAS, Bandar Seri Iskandar 32610, Perak Darul Ridzuan, Malaysia

[10]Division of Electronics and Electrical Engineering, Dongguk University-Seoul, Seoul 04620, Republic of Korea

*Correspondence: ahmad_19001511@utp.edu.my

This is a peer-reviewed, accepted author manuscript of the following paper: Jagaba, A. H., Kutty, S. R. M., Naushad, M., Lawal, I. M., Noor, A., Affam, A. C., Birniwa, A. H., Abubakar, S., Soja, U. B., Abioye, K. J., & Bathula, C. (2022). Removal of nutrients from pulp and paper biorefinery effluent: operation, kinetic modelling and optimization by response surface methodology. Environmental research, 214(Part 4), [114091]. https://doi.org/10.1016/j.envres.2022.114091

Abstract:

This study investigated the effectiveness of extended aeration system (EAS) and rice straw activated carbon-extended aeration system (RAC-EAS) in the treatment of pulp and paper biorefinery effluent (PPBE). RAC-EAS focused on the efficient utilization of lignocellulosic biomass waste (rice straw) as a biosorbent in the treatment process. The experiment was designed by response surface methodology (RSM) and conducted using a bioreactor that operated at 1-3 days hydraulic retention times (HRT) with PPBE concentrations at 20, 60 and 100%. The bioreactor was fed with real PPBE having initial ammonia-N and total phosphorus (TP) concentrations that varied between 11.74–59.02 mg/L and 31–161 mg/L, respectively. Findings from the optimized approach by RSM indicated 84.51% and 91.71% ammonia-N and 77.62% and 84.64% total phosphorus reduction in concentration for EAS and RAC-EAS, respectively, with high nitrification rate observed in both bioreactors. Kinetic model optimization indicated that modified stover models was the best suited and were statistically significant ($R^2 \geq 0.98$) in the analysis of substrate removal rates for ammonia-N and total phosphorus. Maximum nutrients elimination was attained at 60% PPBE and 48 hr HRT. Therefore, the model can be utilized in the design and optimization of EAS and RAC-EAS systems and consequently in the prediction of bioreactor behavior.

Keywords: Ammonia; Extended aeration activated sludge; Pulp and paper biorefinery effluent; Total phosphorus; Response Surface Methodology; Rice straw

1. Introduction

Water and air pollution has always been a persistent issue for most under-developed and developing countries (Toczyłowska-Mamińska, 2017). The flaming of agricultural by - products has been one of the prime contributors of the smoke that creates chaos on roadways and impedes commercial aviation operations from rural airports. When rice is harvested, rice straw is left on the land and cannot be used as animal feeds, so farmers have to burn it. This results in a huge rise in CO_2 emissions, devastating fires, haze creation, and global warming effects. Globally, packaging units are made of single-use paper, wood, cardboard, polypropylene, and other single-use disposable plastic materials (Jin et al., 2013). The notion of a bio-refinery, which converts waste biomass as substrate into a number of diverse commodities, seems prospective for becoming green and making an effect for a healthier and cleaner environment (Umar et al., 2021).

Rice straw and an agricultural residue can be turn into a useful and low-cost organic supply (Wagemann and Tippkötter, 2018). By breaking complex cellulose into its simplified form in the pulp and paper biorefinery, sustainable paper packaging products are produced (Nandiyanto et al., 2017; Naushad, 2014). The packing materials are environmentally friendly and disintegrate organically. The products are harmless to humans and the environment and caters for almost all food types Nevertheless, this industry produces pulp and paper biorefinery effluent (PPBE). The PPBE has the ability to disrupt the surrounding aquatic environment, as well as the vulnerable population, through toxicity, thermal effects, aesthetic issues, and poor biodegradability (Lawal et al., 2021).

Nutrients are wastewater contaminants that cause eutrophication in rivers, lakes, and seas, lowering water quality (Jagaba et al., 2022d); as a result, wastewater discharge poses a constant threat to the global supply of clean water (Stewart et al., 2008). Several treatment plants have recently used increased biological nutrient removal processes to lower nutrient levels in water

and wastewater. Biological nutrient removal comprises increased biological phosphorus removal, biological nitrification, and denitrification (Nath and Bhakhar, 2011). However, all could be accomplished with minor changes to standard activated sludge systems (Al-mahbashi et al., 2022; Lo et al., 1994). Ammonia removal efficiency can be enhanced by increasing wastewater temperature and stream flow velocity, as well as lowering the reflux ratio (Faizal, 2014). Raising the aeration period also increases ammonia removal to a quite a greater extent. This could be attributed to total nitrogen decrease boosting nitrification rate (Al-Rekabi et al., 2017).The removal of phosphorus is an important aspect of wastewater treatment systems (Ayaz et al., 2012; Bawiec, 2019). The effectiveness of phosphorus removal is mostly determined by the hydraulic load and fractionation of daily bioreactors (Dan et al., 2020). The demand for environmentally friendly wastewater treatment and reutilization has increased as water resources continue to be depleted (Kalkan et al., 2011). Thus, the pulping process produces effluent, which can be handled in a number of ways (Assadi et al., 2018; Koupaie et al., 2013; Naushad et al., 2019).

Biological treatment techniques have apparently been used in the treatment of pulp and paper wastewater using aerobic, anaerobic, and aerobic/anaerobic processes (Ahmed et al., 2020; Jagaba et al., 2022a; Noor et al., 2021a; Yu et al., 2015). The conventional activated sludge system has been historically used for industrial wastewater treatment (Ali and Sreekrishnan, 2001). This is due in part, its short hydraulic retention time (HRT), lower capital cost, typically more ecologically friendly, and fewer operational requirements than other physical processes. The AS system is made up of the aeration tank, the settling tank, and the sludge recirculation (Jagaba et al., 2022b). It is the most common biological treatment method (Ng et al., 2021). AS wastewater treatment facility can remove biological inorganic and organic substances depending on the design and use(Mareai et al., 2020). The AS now comes in a variety of tweaks and variations to address these flaws, one of which is extended aeration system (EAS).

There is an increased focus by scientist and engineers on the use of EAS in wastewater treatment in combination with a range of biosorbents. However, the biosorbents that are suitable for use in the adsorption systems must be cost-effective. They should also be reusable, have a high biosorption efficacy, and have quick biosorption kinetics (Zhou et al., 2018). Environmentally safe materials such as biomass based activated carbon have recently been employed for pollutants biosorption (Mo et al., 2018; Xiao et al., 2019). Rice straw has long been utilized as a biosorbent in various forms (Rosales-Calderon and Arantes, 2019).

Wastewater treatment with activated carbon biosorption is a commonly used treatment method (Jagaba et al., 2019). The bulk of organic molecules in water may be highly absorbed into the activated carbon because of the appropriate surface area and micro pores (Tahir et al., 2016). To remediate an industrial wastewater, it was demonstrated that incorporating PAC to a system might remove antibiotic compounds and, as a result, improve removal efficiencies over a system without PAC (Jaafarzadeh et al., 2010). This was indeed attributable to activated carbon's biosorption capacity that provided a large surface area with many holes for refractory nutrients removal (Noor et al., 2021b; Wang et al., 2016).

This study attempts to provide a novel approach that highlights the feasibility of simultaneous biosorption and biodegradation of nutrients from field based PPBE in both EAS and RAC-EAS bioreactors. The objectives that guided this study were to: (i) characterize the PPBE, and RAC (ii) optimize the EAS and RAC-EAS treatment processes by RSM (iii) evaluate the effect of HRT, PPBE concentration and RAC on nitrification rate, Ammonia-N and TP degradation efficiency under continuous-flow conditions, and (iv) determine the best kinetic models based on performance.

2. Materials and Methods

2.1. Materials

All chemicals used during the study were of the highest purity. Rice straw biomass was obtained from a local company operating in the neighboring area of Seri Iskandar, Tronoh,

Perak, Malaysia. Bonded pollutants were eliminated by regularly scrubbing the rice straw with clean water. For 24 hours, cleansed rice straw was soaked in 1 L/100 g mineral water. The rice straw was then cleaned with a solvent and subsequently with mineral water and air dried for 24 hours at 110ºC in an oven. After drying, the sample was reduced to 2.5–5.0 mm in size using a mechanical granulator. Using a mechanical grinder (Fig. S1), the rice straw was ground to 75 µm powder. The PPBE used was sourced from a firm in Gurun, Kedah, Malaysia. Rice straws and husks are used to make biodegradable food packaging materials at this enterprise.

2.2. RAC biosorbent preparation

Carbonization was carried out in a horizontal tube furnace (OTF-1200X, MTI Corporation, USA) to manufacture activated carbons. 30 g of pretreated rice straw was immersed in 0.1 M HCl for 24 hrs to make the substrate. This was undertaken to clear the material of contaminants that could interfere with the bio-sorption process. Mineral water was then used to wash the treated samples. The substrate was heated for 2 hours at 750°C at 10°C/min in a tube furnace. After reaching the desired temperature, argon was substituted with N_2 at a flow rate of 5 L/min for activation and kept on hold for a duration of 1 h. The N_2 was added to the air to lower the oxygen concentration and avoid agglomeration and stacking during the heating process. The samples were allowed to cool before being stored in a sealed jar to avoid pore obstruction due to ambient gas adsorption. The synthesized carbons were smashed and permeated prior to it's use in a bioreactor (Birniwa et al., 2021; Tummino et al., 2019).

2.3. RAC characterizations RAC biosorbent was characterized. The N_2 adsorption–desorption with Micrometric ASAP 2020 was used to determine the BET surface area and pore size of the RAC. The Field emission scanning electron microscopy (FESEM) was used to determine the RAC morphology using Zeiss supra 55 VP instrument (Naushad, 2014). The high-resolution micrographs of the FESEM image were achieved at different kx magnifications on an

accelerated voltage of 200 kV and the samples were sputter-coated with Au metal before the imaging analysis. The functional group of the RAC was obtained by scanning the spectral range of 400 to 4000 cm^{-1} on a Perkin Elmer FTIR Spectrometer using the KBr pellet method. The attenuated total reflectance mode is used as a sample injection to examine functional groupings. The proximate value tests, greater heating value, ultimate analysis and moisture content test were carried out in accordance with ASTM E1755-01, D4809-00, ASTM D3176-09 and ASTM E871-82, respectively. They were conducted using the LABsys Evo TGA analyzer, Ac-350 bomb calorimeter, and Leco CHNS-932 type analyzer.

2.4. Bioreactor properties, fabrication, and operation

The experimental process began with the design and fabrication of an extended aeration bioreactor system. The bioreactor setup has an influent tank that is coupled to the aeration tank through a tube driven by an up-flow pump, while the treated overflow released into an effluent tank. Schematic diagram of the EAS and RAC-EAS bioreactor set-up is depicted in Fig. S2. Details on the bioreactor properties are provided in the supplementary information section. The following parameters are being measured: Ammonia-N, TP, nitrate, nitrification rate, MLSS and MLVSS.

2.5 Analytical methods

Standard procedures for the investigation of water and wastewater were used to obtain all experimental measurements in a steady state operation of the system (Jagaba et al., 2021a). Every measurement was carried out three times. Daily measurements of DO and pH were taken. Standard Methods were used to analyze MLSS and MLVSS (APHA, 2005) (Mohammadi et al., 2011). The performance efficiencies of the bioreactors were determined using equations 1.

$$\text{Removal efficiency } (\%) = \frac{E_o - E_e}{E_o}\ x\ 100 \text{ ----------(1)}$$

Also, ammonia loading rate, nitrification rate (NR), and HRT were determined using Eqs. (2–4), respectively

$$\mathrm{NR} = \frac{[\mathrm{NH_4^+{-}N}]_{inf} - [\mathrm{NH_4^+{-}N}]_{eff}}{VS\ x\ T} \text{ ----------(2)}$$

$$\mathrm{HRT\ (h)} = \frac{v}{Q} \text{ ----------(3)}$$

$$\mathrm{NH_4^+ - N\ loading\ rate}\ (\frac{\mathrm{mg}}{\mathrm{L}}.\mathrm{h}) = \frac{(Eo)Q}{V} \text{ ----------(4)}$$

Where T = reaction time (h), V = volume of the bioreactor (m^3), Q = water flow rate (L/d), E_o and E_e are initial and final Ammonia-N and TP concentrations (mg/L) (Zhang et al., 2017).

The reported data was the standard deviations of average of three replicates. The generated data was analyzed by Origin software. Analysis of variance (ANOVA) was used to compare the means of three replicates, and the results were evaluated at the 0.05 level (p0.05) (Shitu et al., 2020).

2.6. EAS and RAC-EAS optimization by RSM for Ammonia-N and TP removal

. Central composite design was utilized to acquire the optimal experimental data perfect blend from the initial one-factor-at-a-time trials using this model (Asfaram et al., 2015; Jagaba et al., 2022c; Saeed et al., 2021). Optimum mixes to enhance contaminant removal rate were tested using numerical optimization. The effects of two process factors, PPBE concentration and HRT, were examined. These parameters were selected due to their significance in the reactor operation and substrate degradation. The variables investigated for this design were PPBE concentrations that varied from 20 to 100% and HRT varying from one (1) to three (3) days (see Table S1). Details describing the optimization model performance are provided in the supplementary information section.

2.7. Kinetic study

Biokinetic models are commonly used to assess experimental values to examine the biosorption mechanism and its potential phases of rate regulatory actions. Several kinetic models have been used by scientists. The Modified Stover–Kincannon, First, and Second-order kinetic models were used in this study to estimate the biosorbent uptake rate and confirm the limiting stages in the biosorption process. Detailed procedures and relevant equation for each model are explained in the supplementary section.

2.8. Biosorption mechanism for activated carbon in RAC-EAS

In a simultaneous biosorption and biodegradation process, activated carbon is placed in aeration tank as in standard industrial practice (Korotta-Gamage and Sathasivan, 2017). The interplay of biosorbent particles, microbes, pollutants, and DO in aqueous solution is illustrated in Fig. S3 as the RAC mechanism for substrate removal. Details of the process mechanism is described in the supplementary information section

3. Results and discussion

3.1. Influent PPBE characteristics

The fresh PPBE samples had high levels of nutrients that exceeded standard industrial discharge limit. The increased load of organic substances with bacterial activity is reflected in the elevated concentration of BOD_5 in the wastewater. It also demonstrates the possibilities of treating wastewater with biological processes. The COD content in wastewater indicated the presence of oxidizable organic matter. This reflects the possibility of using biosorption process with promising prospects to disintegrate low, medium, and high-strength wastewater concentration, especially when biomass materials are considered as the biosorbents. The fresh influent PPBE characteristics were 8.2 pH, 25.4ºC temperature, 1194 mg/L TDS; 682 mg/L TSS;

5004 mg/L COD; 2117 mg/L BOD_5; 56.2 Ammonia-N; 0.53 Nitrate; 143 TP (mg/L), 164 NTU and turbidity.

3.2. Characteristics of RAC

3.2.1. Chemical composition RAC

X-Ray fluorescence spectroscopy was used to examine the RAC components. Table S2 showed the chemical composition of RAC. The cumulative percent compositions of Al_2O_3, SiO_2, and Fe_2O_3 for the RAC is 69.07%. CaO and Cl were found in 0.75% and 0.77% of the RAC respectively. A study by (Maged et al., 2021) also reported an increase in SiO_2 in a modified material. It's worth noting that the quality of activated carbon made from biomass is mostly determined by its high SiO_2 content. The findings acquired were similar to those published by (de Palma et al., 2021). On the analysis of rice straw, the RAC investigated in this study shared chemical features with numerous biosorbents derived from biomass materials that have been earlier utilized in biological treatment systems for biosorption.

Table 1 showed the RAC elemental composition determined by EDX. All items were evaluated under the "Normalized" processing option. Cl, Si, K, Ca, and P are the RAC's most important elements. The element K was discovered to be the most abundant. The presence of starch in the raw ash was responsible for the high concentration of Ca and Si recorded. All of which aided in pore creation and hence the biosorption process. A study published by (Imran and Khan, 2018) found similar results. Ca and Si are both important components in nutrient removal. The findings suggested that RAC as a biosorbent has a great potential for eliminating contaminants throughout the biological treatment process.

Table 1. Elemental composition of RAC

Elements	Ca	Rb	K	Zn	Cl	Cu	Fe	P	S	Mn	Si
Values (%)	24.4	0.27	49.6	0.68	7.83	0.52	2.32	7.12	2.47	0.59	4.2

3.2.2. FESEM

RAC morphology was evaluated using FESEM, as depicted in Fig. S4a and b. The image was taken at a magnification of 30000-50000 times and analyzed using Energy Dispersion Spectroscopy (EDS). The RAC revealed a sieve-like structure with heterogeneous and vastly porous openings and honeycomb surfaces that are like a lettuce shape with no tendency to form aggregates that have the potential to trap contaminants. This was an indication that the pretreatment eliminated exterior fibres, increasing surface area, and making cellulose within reach to enzymes. The RAC particles plated with sharp edges, aggregated easily due to its free-flowing characteristics, and became porous and loose. These findings are consistent with that reported by (Pereira et al., 2014).. Rice straw prepared with electron beam irradiation and rice straw prepared with aqueous ammonia soaking, exhibited structural changes that were similar (Borba et al., 2021; Nandiyanto et al., 2017). According to the EDX spectrum depicted in Fig. S4c, Potassium, oxygen, carbon, and silicon had concentrations of 0.17, 18.38, 76.56, and 4.88 wt%, respectively.

3.2.3. RAC specific surface area (SSA) and porosity

Macropores (d > 50 nm), mesopores (2 nm < d < 50 nm), and micropores (d <2 nm) are the three types of pores classified by the International Union of Pure and Applied Chemistry (IUPAC). The pore diameter of the substance is denoted by the letter "d". Table 2 depicted that RAC has an SSA, pore volume, micropore surface area and pore size of 1203.7 m^2/g, 0.449 (cm^3/g), 1172.2 m^2/g and 187.4 (Å), respectively. This is consistent with findings by (Sarkar et al., 2020). The quantity of micropores in the RAC was discovered to be adequate. This might be linked to complexation and graphitization because of the carbonation process. The RAC belonged to the mesopores material class, as per the IUPAC classification. Itis probable that the RAC's massive surface area influenced the thermal treatment associated with the process. As a result, the average pore size of the material increased gradually. Review of recent literature indicated that

the surface area of certain treated rice straw was found to be higher than produced RAC. This could be linked to the differences in rice straw varietals and other treatments done to activated carbon besides heating (Rasheed et al., 2020).

Table 2. The RAC physical properties.

Parameter	BET surface area (m^2/g)	Micropore surface area (m^2/g)	Total pore volume (cm^3/g)	Micropore volume (cm^3/g)	Average pore size (Å)
Values	1203.7	1172.2	0.449	0.412	187.4

3.2.4. RAC ultimate and proximate analysis

The study examined the pH, ultimate and proximate analysis for the samples of RAC to discover the biosorbent chemical ingredients for use in the RAC-EAS system for the PPBE treatment. Results of proximate analysis indicated that, RAC has a high volatile matter and fixed carbon content. This could result to obtaining high calorific value. The high percentage of volatile indicated that RAS is inorganic in nature and was further proven by its high amount of carbon content. The high value obtained for the fixed carbon could be due to the conversion of volatile matter of the raw rice straw into fixed carbon during the carbonization process. Proximate analysis results indicated that, carbonization of the rice straw has enhanced the quality of the produced RAC. Despite obtaining high volatile matter, some are said to have been converted to gaseous products and RAC had huge ash content. The presence of high ash content indicates its poor combustion status and increase in burning time. The values obtained are in agreement with findings by (Nam et al., 2018). The moisture contents found in this investigation matched with those attained by (Nasara et al., 2021) and (Alhassan et al., 2018). According to the proximate analysis, carbonization of the rice straw has enhanced the quality of the produced RAC. The RAC's high SO_2 content of 74% has very much proven the material's durability. The

ultimate analysis of RAC with result depicted in Table S3 was undertaken to analyze the elemental compositions.

3.2.5. FTIR

A biosorbents sorption capacity is mostly determined by the existence of functional groups in the material. The removal of hemicelluloses and alteration of the lignin structure induced various compositional and structural changes adjustments to the treated materials because of the thermal treatment. RAC FTIR pattern before the biosorption process is illustrated in Fig. 1. This was undertaken to discover the functional groups present in the biosorbent. It has bands at 3411.65, 2342.36, 1581.26, 1085.47, and 472.93 cm^{-1} respectively. In comparison with results of raw rice straw in literature, the absorbance peaks in the RAC were larger. The concentration of free and intermolecular bound defines the significant peak at 3411.65 cm^{-1}, which illustrates the existence of phenol groups. A pronounced adsorption band at 1581.26 cm^{-1} could be attributed to the C=C stretching vibration of the phenol group in aromatic rings. The presence of OH and NH groups, as well as C-N to C-H stretch, imply carboxylic group deformation at 1085.47 cm^{-1} (Abubakar et al., 2016). Aromatic – carbon-carbon rocking waves are the primary drivers of 472.93 cm^{-1} aromatic bands. Methylene and methyl, as well as aromatic rings, are hydrophobic groups in the RAC. As a result, they are referred to as highly hydrophobic (Azmi et al., 2016).

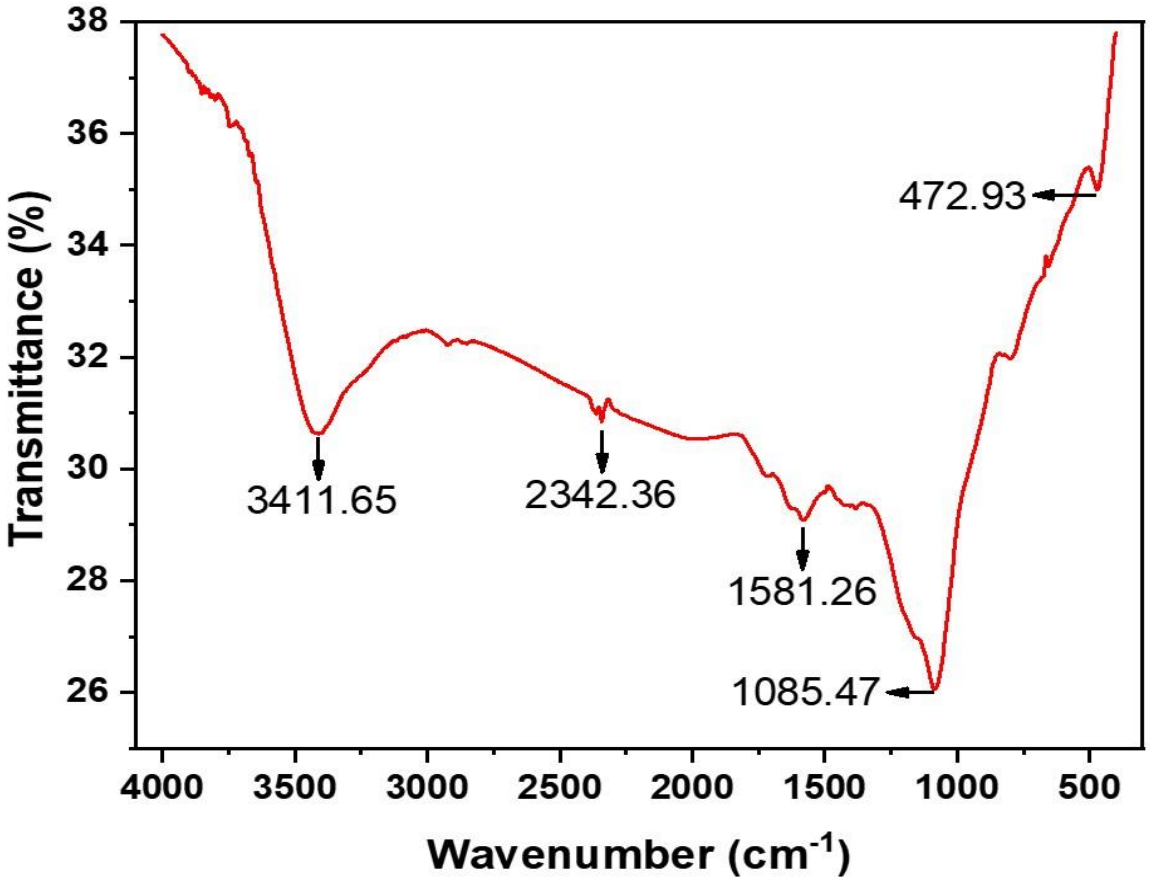

Fig. 1. FTIR spectrum of RAC.

3.3. Performance evaluation of RSM optimized EAS and RAC-EAS bioreactors for PPBE treatment

In developing and assuring the economic feasibility of bioreactor running, the optimal time and circumstances for achieving the target threshold of contaminant removal are critical. The effects of various HRTs and wastewater concentrations on the efficiency of newly constructed bioreactors were investigated in this work, as well as the protracted functionality of both bioreactors. The operational HRT was gradually shortened from 3 days to 2 days to 1 day. Table S4 described the bioreactors (EAS and RAC-EAS) operational duration ranging from 0-224 days along with MLSS and MLVSS values at each HRT. The bioreactors were run up until substantially stable states were reached, at which point the biomass's embedded bacteria acclimated to the environment. The table also highlights the influent and effluent concentrations

of PPBE. At the initial stage of the experiment, it could be observed from the table that the reactor operated for 0-45 days. The first 15 days were for acclimatization, while the subsequent 30 days were for the 3-day HRT period. Table 3 highlights all the runs within the experimental design matrix, independent variables (HRT and PPBE %), and obtained values for responses (Ammonia-N, TP, and nitrification rate).

Table 3. Design matrix for nitrification rate, Ammonia-N, and TP removal.

Run	**Design of experiment (DOE) for the optimization of nitrification rate, Ammonia-N, and TP removal**							
	Independent variables		**Responses**					
			EAS			**RAC-EAS**		
	PPBE (%)	HRT (days)	NH_4^+-N removal (%)	TP removal (%)	Nitrification rate ($mgNH_4^+$-N/mgVSS/d)	NH_4^+-N removal (%)	TP removal (%)	Nitrification rate ($mgNH_4^+$-N/mgVSS/d)
3	20	3	76.61	69.71	0.0068	83.13	79.23	0.0069
6	60	3	62.5	76.55	0.0209	89.02	81.07	0.0280
8	100	3	59.62	55.60	0.0381	74.94	68.92	0.0450
1	100	2	74.19	69.15	0.0176	76.60	69.79	0.0307
4	60	2	84.51	77.62	0.0186	91.71	82.74	0.0185
7	60	2	82.84	72.66	0.0039	89.90	83.54	0.0180
10	60	2	79.38	70.03	0.0175	91.03	84.64	0.0172
11	20	2	69.13	62.32	0.0329	88.86	79.68	0.0048
2	20	1	62.23	74.49	0.0019	87.75	78.01	0.0024
5	60	1	68.29	77.41	0.0074	89.81	81.93	0.0086

9	100	1	62.48	57.63	0.0134	70.16	68.15	0.0127

3.3.1. Parameters process optimization for Ammonia-N and TP removal

The 3-D surface plots were made using design expert software by maintaining one property constant while charting the graph in relation to another. Ammonia-N removal effectiveness ranges from 74.19% to 84.51% and 70.16% to 91.71 for EAS and RAC-EAS respectively. TP removal efficiencies ranges from 55.60% to 77.62% and 68.15% to 84.64% for EAS and RAC-EAS respectively. The highest nitrification rates were 0.0381 and 0.045 for EAS and RAC-EAS respectively. Fig. S5 and S6 show a 2-D contour plot and a 3-D surface plot of nitrification rate, Ammonia-N, and TP removal from bioreactors, respectively. They demonstrate the influence of PPBE concentration and HRT all through the experiment following DOE optimization. The nutrient input rate was modified when the bioreactor stabilized. The highest value achieved after optimization was 84.51.71 percent and 77.62% for Ammonia-N and TP elimination at MLSS and MLVSS values of 4014.81 mg/L and 3400.60 mg/L respectively. At MLSS and MLVSS values of 4240.74 mg/L and 3640.97 mg/L, respectively, the RAC-EAS had a highest value of 91.71% and 84.64% for Ammonia-N and TP removal at a 60% PPBE concentration after two days of HRT. The system's findings indicate that the population of microbes absorbing nutrients is quickly rising. Toxic compounds in the PPBE attempted to impede with the microbial population's functioning, resulting in lower efficiency. Further studies and analysis are highly required, however, to examine the impact of these substances on nutrient degradation process. A study by (Tsang et al., 2006) measured an 81.63% removal efficiency from a TP influent comprising 149–572 mg/L. With an 83% eradication rate, this result was consistent with the conclusion drawn from the above mentioned study. The variance could be explained by other PPBE elements, and also the level of TP concentration in the influent. For the EAS and RAC-EAS aerobic bioreactors, the HRT plays a significant role in Ammonia-N and TP elimination.

The elimination efficiency increased in terms of the rate of biomass contained. The bioreactor exhibited organic overloading when the PPBE content rises to 100%, resulting in a drop in microbe intake (Liang et al., 2021). It is really noteworthy that removal rate has increased in response to MLSS feed, which is in line with earlier study by (Cai et al., 2019). It can be deduced from the pattern that when the contact time of biomass in the reactor is increased, more degradation occurs, leading to increased nutrient removal. However, when the cycle length was lowered from 3 days to 1 day, the removal effectiveness for both Ammonia-N and TP systems decreased after 2 days. This consequently led to reduced nitrification rate. This may be deduced from the observation that the longer biomass contact time with the nutrient in the system (three days) had an impact on the nutrient removal efficiency. In both bioreactors, Ammonia-N was eliminated in relation to HRT (days). Ammonia-N was absorbed and stabilized in the effluent in the range of 11.74–31.93 mg/L because activated sludge is the principal consumer of organic and nutritional constituents in the system. Other studies treating pulp and paper wastewater by (Farooqi and Basheer, 2017) and (Adel et al., 2020) have reported about 61%, 78% and 79.7% ammonia reduction respectively. Nonetheless, when the EAS reactor was used, an effective removal of 91.71% was accomplished with an average ammonia influent concentration of 35.41 mg/L in the sample. The efficiency of nutrient removal in biological nutrient removal processes (BNR) is related to the type of influent feed (Naushad, 2014).

The RSM model was used to obtain the expected versus actual values. The real data and the model's predicted data are comparable, as shown in Figs. S7 and S8 for EAS and RAC-EAS, respectively.The equations 5 - 7 for the polynomial regression model for EAS and equations 8-10 for RAC-EAS are as follows:

$$\text{Ammonia-N removal (\%)} = +78.68 - 5.08A + 0.9550B - 4.31AB - 1.68A^2 - 12.27B^2 \quad (5)$$

$$\text{TP removal (\%)} = +73.92 - 6.89A - 1.28B + 0.6875AB - 8.91A^2 + 0.5839B^2 \quad (6)$$

$$\text{Nitrification rate} = +0.0178 + 0.0120A + 0.0072B + 0.0049AB - 0.0007A^2 - 0.0035B^2 \quad (7)$$

$$\text{Ammonia-N removal (\%)} = +91.36 - 6.34A - 0.1050B + 2.35AB - 9.34A^2 - 2.66B^2 \quad (8)$$

TP removal (%) = +83.43 - 5.01A + 0.1883B - 0.1125AB - 8.39A^2 -1.62B^2 ---------- (9)

Nitrification rate = +0.0182 + 0.0124A + 0.0094B + 0.0069AB - 0.0009A^2 -0.0003B^2 -------- (10)

The equation in terms of coded factors is being utilized to provide response projections for specified levels of every component. The maximum levels of the components are coded as +1, while the small fractions are coded as -1. By correlating the component coefficients to the factor coefficients, the coded equation could also be utilized to find the exact effect of the components. Table S5 illustrates the real equations for NR, Ammonia-N, and TP removal.

3.3.2. Quadratic models (ANOVA) for Ammonia-N and TP removal

The inclusion of the software's optimization feature provides for the evaluation and implementation among the most relevant values in real-world applications. In this study, nitrification rate, Ammonia-N and TP removal were optimized by adjusting the input factors. Given statistically significant conditions, the experimental model accuracy created by the RSM technique is evaluated using ANOVA. According to the constructed model, when a substantial value of F-index is relatively small and the P-index is low, the model is statistically significant. Failure of the model to fulfil experimental with modelled parameters should be minor.

Table S6 show the ANOVA results for the modelled response variables. The table reveals that the Model F-values of 62.87, 5.42 and 6.0 for NR, Ammonia-N and TP removal respectively in EAS while 104.87, 103.01 and 483.89 were achieved for nitrification rate, Ammonia-N and TP removal respectively in RAC-EAS. This indicated that the model is essential.

In EAS, there was 0.02%, 3.56%, and 4.35% chance that an F-value this significant might arise due to noise for NR, Ammonia-N, and TP elimination, respectively. The F-values of 0.76 and 0.77 for Ammonia-N and TP removal, respectively, suggest that the Lack of Fit was insignificant in comparison to the pure error. There are 61.21% and 60.89% chances for Ammonia-N and TP that a Lack of Fit F-value this large could take place due to noise. To

genuinely model the variables to fit, a small lack of fit is acceptable. The Lack of Fit F-value of 17.94 for NR indicates that a large Lack of Fit F-value could occur owing to noise 5.32% of the time. However, Lack of fit (less than 10%) is concerning. In RAC-EAS, there is only a 0.01% chance each for NR, Ammonia-N and TP removal, that an F-value this huge could develop as a result of noise. The F-values of 1.45 and 0.65 for Ammonia-N and TP removal, respectively, indicated that the Lack of Fit was not significant in comparison to the standard error. For Ammonia-N and TP, there are 43.28% and 65.39% possibilities, respectively. The Lack of Fit F-value of 1.96 for NR suggests that a significant Lack of Fit F-value could occur owing to noise 35.48% of the time. Inessential lack of fit is acceptable.

Tables S7 and S8 described the model comparison, fit and statistics. Table S8 shows that the Predicted R^2 values of 0.8391, 0.1032, and 0.2360 for NR, Ammonia-N, and TP removal in EAS are reasonably consistent with the Adjusted R^2 values of 0.9687, 0.6887, and 0.7144 for NR, Ammonia-N, and TP removal, respectively. The discrepancies all seem to be less than 0.2, as can be seen. Adeq Precision measures the signal to noise ratio, and a value > 4 is ideal. The proportion of 25.513, 7.318, and 5.537 for NR, Ammonia-N and TP elimination accordingly demonstrates appropriate signal. This showed that the models can be used at different design domain.

In RAC-EAS, R^2 values of 0.9856, 0.9484, and 0.9471 for NR, Ammonia-N and TP removal respectively, and conforms with the findings of the Adjusted R^2 values of 0.9959, 0.9811 and 0.9808 for NR, Ammonia-N and TP removal respectively. The discrepancies all seem to be less than 0.2. Adeq Precision measures the signal to noise ratio, and a value > 4 is ideal. The NR, Ammonia-N, and TP elimination ratios of 71.483, 27.050, and 24.126, respectively, suggest appropriate signal. This shows that the models can be used at different set of design domain to another. The coefficient estimate readings in Table S9 represent the expected variation in response per unit change in factor value once all factors remain constant. The VIFs are 1 when the factors are orthogonal; VIFs more than 1 imply multi-collinearity; the

higher the VIF, the more intense the factor correlation. VIFs of fewer than ten are considered tolerable. Fig. S9 illustrates the removal ramps and desirability solution for nutrient removal generated by a design expert using modelled parameters after optimization, with values of 0.666 and 0.754 for EAS and RAC-EAS, respectively. For PPBE concentration and HRT, the optimization ramp demonstrates the attractiveness of dependent variables. So, each dot on the ramp represents the desired variable and response behavior target.

3.4 Impact of PPBE concentration and HRT on Ammonia-N removal, nitrate accumulation and NR

3.4.1 Ammonia-N removal and nitrate accumulation

The prevalence of nitrifying bacteria, that consumes ammonia and produce nitrate through an oxidation reaction, predicted the removal of nitrogen molecules through biological processes. Increasing the retention duration in an EAS results in improved nitrogen compound utilization than activated sludge (Mareai et al., 2020). The treatment should ideally be able to remove significant amount of nitrogen from the influent.

The initial experiments evaluated nutrient removal in EAS and RAC-EAS augmented with activated carbon particles. Fig. 2a shows a comparison between EAS and RAC-EAS as regards effluent Ammonia-N concentration based on distinct PPBE concentration (20-100%) and HRT (24-72 h) as already explained in the methodology with influent Ammonia-N concentration ranging from 11.43-58.37 mg/L. The figure also showed the varied NH_4^+-N concentrations in the two bioreactors, along with their biosorption capacities. Table 4 shows the average NH_4^+-N treatment efficiency, with the average effluent NH_4^+-N concentration of the bioreactors been extremely low. The conversion potential of ammonia to nitrate was intensified in both reactors with relatively insignificant nitrite generation (less than 0.1 mg/L) all through the operation phases. It was also established that the 60% PPBE concentration resulted in a lower Ammonia-N

concentration in the effluent of the two systems, but the 100% concentration resulted in an increase in Ammonia-N concentration. In this study, prolonged HRT (72 h and 48 h) was found to have the highest ammonium elimination effectiveness when compared to a lower HRT of 24 h. Ultimately, a 48-hour HRT was indicated as the best HRT for successful Ammonia-N removal for the PPBE treatment in both EAS and RAC-EAS bioreactors from both an economic and ecological standpoint. In addition, the figure showed that, adding RAC to the RAC-EAS bioreactor resulted in a greater reduction in effluent Ammonia-N concentration. Supplementing RAC to a bioreactor, as expected, enabled further nitrogen component removal by combining the benefits of biodegradation and adsorption(Jagaba et al., 2022d). During the 224-day operation, the RAC-EAS removed NH_4^+-N at a rate of up to 98.15%. There was no discernible variation in NH_4^+-N removal efficiency seen between two bioreactors, as shown in Table 4. As a result, the RAC had little effect on NH_4^+-N elimination. The increase in Ammonia-N removal in the addition of RAC particles was linked to increased biomass and granulation. By reducing the start-up period while adding RAC particles, near-complete and steady Ammonia-N removals were achieved. In the RAC-EAS, ammonia elimination was steadily developed, enhanced, and attained around 90% by day 146. Following that, the removal performance remained nearly constant until the experiment's conclusion (152 days). Ammonia removal was developed quickly in the RAC-EAS enhanced bioreactor, with a start-up time of only 7 days. The process was stabilized at 75%. From day 33 onwards, there was efficient and consistent Ammonia-N elimination of greater than 94%. In RAC-EAS, Ammonia-N was largely eliminated during the aeration phase. While both reactors were run together under the circumstances, the nitrogen removal accomplished in RAC-EAS was around 1% greater than in EAS. As a result, the RAC altered the mass transfer of nutrients and substrates to the biomass-embedded microbial population. Furthermore, the substrates' dispersion into RAC was influenced by the biomass's flow velocities. Larger localized concentration gradients and higher rates of diffusion forward through biomass emerged from any increase in flow velocity. Moreover, the aeration flow is

connected to the flow velocity in aerated bioreactors. The aeration flow not only adds DO to the system, but it also allows RAC to roam around (Zhang et al., 2017).

The bioreactors utilized for the study showed good stability when subjected to hydraulic and substrate shock loads caused by increased influent flow rates. This discovery could be understood more by the biomass' age and stability, as well as the structure and characteristics of the RAC involved. The concentrations of NH_4^+-N and NO_3^--N in the effluent of the EAS reactor constantly reduced and increased. The rate of growth in NO_3^--N, on the other hand, is slower. Unlike NH_4^+-N, there was no evidence of NO_2^--N accumulating in both bioreactors, which were reported to be at low concentrations of <0.5 mg/L. Regarding nitrite buildup, neither bioreactor showed a significant difference. The results showed that nitrite-oxidizing bacteria grew successfully in both bioreactors, with considerable nitrite-to-nitrate oxidation capabilities. Fig. 2b presents the influent and effluent nitrate concentrations in both EAS and RAC-EAS based on different PPBE concentration. Although, effluent concentrations in both bioreactors were way higher than the influent, it could be observed that less nitrate concentration was recorded for the RAC-EAS as compared to the EAS bioreactor (Mareai et al., 2020). During initial days of the experiment, low NH_4^+-N removal efficiency was observed. This finding indicated that NH_4^+-N oxidation is a somewhat sluggish process. Remarkably, both bioreactors revealed the potential to highly oxidize the target ammonium within 146-152 days of the continuous flow experiment. With the continued operation of the bioreactors, the removal efficiency of NH_4^+-N was improved with time, with recorded maximum values of 84.51% for EAS and 91.71% for RAC-EAS attained. This could be attributed to the dramatic rise in hydraulic shear stress imposed on the biomass, which certain microbe species are unable to endure (Shitu et al., 2020). A decrease in bioreactor effectiveness may be caused by a mass transfer bottleneck caused by a decrease in contact time seen between influent and biomass. The effluents of EAS had nitrite all through start-up, inferring ammonia nitrification and partial TN removal. However, due to excellent TN removal, no nitrite or nitrate was observed in the effluents after the start-up. During Ammonia-N

removal in RAC-EAS, the emission of nitrite and nitrate into the bulk liquid was negligible at steady state. Because of excellent TN removal, nitrite and nitrate concentrations in RAC-EAS effluents were not noteworthy from the start. In the introduction of RAC particles, the start-up times for establishing efficient N removal were reduced.

3.4.2 Nitrification performance rate

Continuous flow experiment was carried out for 224 days to evaluate the nitrification performance of EAS and RAC-EAS bioreactors. This study reported on the nitrification performance in PPBE treatment in two bioreactors. Fig. 2c shows the time course concentrations and nitrification rate throughout the experimentation period. It revealed good nitrification rate from day 16. The whole nitrification reaction may have been aided by improved aerobic environment in both bioreactors (Jagaba et al., 2022c). Both bioreactors' nitrification capability increased rapidly, with excellent ammonium removal. The initial assessment suggested that as the HRT decreased, the nitrification effectiveness of both EAS and RAC-EAS somewhat decreased. However, it promptly healed after many days of continuous operation up until the moment of attaining constant circumstances which culminated in a good effluent Ammonia-N concentration. In both bioreactors, a reduction in influent retention time was observed to impair the achievement of high nitrification performance. Ammonia-N may still be a constraining element for the nitrification process as HRT increases. As a result, a higher nitrification rate is a strong indicator of the nitrification process' efficacy. The findings also suggested that the presence of RAC had no major impact on the nitrification rate. The somewhat higher nitrification rate on the mean was seen in RAC. The maximum elimination efficiency for RAC-EAS was achieved after 48 hours of HRT, which was higher than the results of previous investigations. Furthermore, the bioreactors' strong nitrification performance at a shorter retention time could be connected to the bioreactors' longer operation, which favors nitrifying bacteria proliferation. For both EAS (0.019 mgNH_4^+-N/mgVSS/d) and RAC-EAS (0.0086 mgNH_4^+-N/mgVSS/d),

shortened HRT resulted in the highest average NR. According to the findings of this investigation, the RAC-EAS had a higher NR than the EAS. In bioreactors, however, the NR dropped as the biomass volume increased. Based on the findings, RAC is recommended for both EAS and RAC-EAS systems with high NRs of 0.0039 mgNH_4^+-N/mgVSS/dand 0.0180 mgNH_4^+-N/mgVSS/d, respectively.

3.4.3 Effect of PPBE concentration and HRT on TP removal efficiency

The effects of PPBE and HRT on the efficiency of bioreactors (EAS and RAC-EAS) in terms of TP removal were studied, and the results are shown in Fig. 2d. It could be seen in the results that both EAS and RAC-EAS were able to remove TP from the PPBE, however the RAC-EAS bioreactor obtained a greater reduction in effluent TP concentration. TP removal increased gradually during the start-up period of both bioreactors, eventually stabilizing at around 41% and 73% in EAS and RAC-EAS, respectively. Because of the establishment of bio-P removal, the TP concentration in the effluents became lower than in the influents. TP concentration in the effluent water for 60% PPBE, ranged from 20.11 to 29.68 mg/L for EAS and from 19.36 to 24.39 mg/L for the RAC-EAS system. This result was expected due to the combined effect of RAC presence as well as the application of higher detention time in the RAC-EAS bioreactor. It can be noticed that the addition of PPBE up to 100% into the bioreactors had an adverse impact on their performance resulting in decreased TP removal. When the increased concentration of TP in PPBE was 156.05 mg/L, the TP content in EAS effluent reached 73.46 mg/L. The RAC-EAS system followed the same pattern. However, at 155.97 mg/L influent TP, the effluent TP concentration reached 55.59 mg/L. This conclusion could be explained by the buildup of TP in bioreactors, which inhibits the action of microbes, specifically when the wastewater lacks all of the nutrients essential for microbial growth.

The removal efficiency of TP in the EAS bioreactor was 77.62% at 2 days HRT for 60% PPBE. This percentage slightly decreased to be 76.55% when the HRT was changed to 3 days at

same PPBE concentration. Similarly, TP removal efficiency in the RAC-EAS bioreactor was 84.64% at 2 days HRT for 60% PPBE. This percentage decreased to 81.07% when the HRT was changed to 3 days at same PPBE concentration. Comparatively, TP removal was more stable in RAC-EAS using RAC particles. At 100% PPBE concentration, however, phosphorus removal efficiencies remained lower. Altogether, TP removals in the RAC-EASS were 1.7–2 times greater than in the EAS. As previously stated, RAC-EAS outperformed EAS in terms of TP removal in all phases studied, even at the highest added influent PPBE concentrations. It's worth noting that adding activated carbon to the RAC-EAS bioreactor slightly improved the TP removal efficiency. This enhancement could be attributed to RAC's adsorption process, which offers a large surface area with multiple holes for the removal of refractory organics. Furthermore, the RAC particles served as a medium for microorganism adhesion and growth (Shitu et al., 2020). Meanwhile, a similar observation was made by (Wang et al., 2016)] and (Sarvajith and Nancharaiah, 2022) where for higher reduction in both TP and Ammonia-N from wastewater when an activated sludge system was combined with powdered activated carbon.

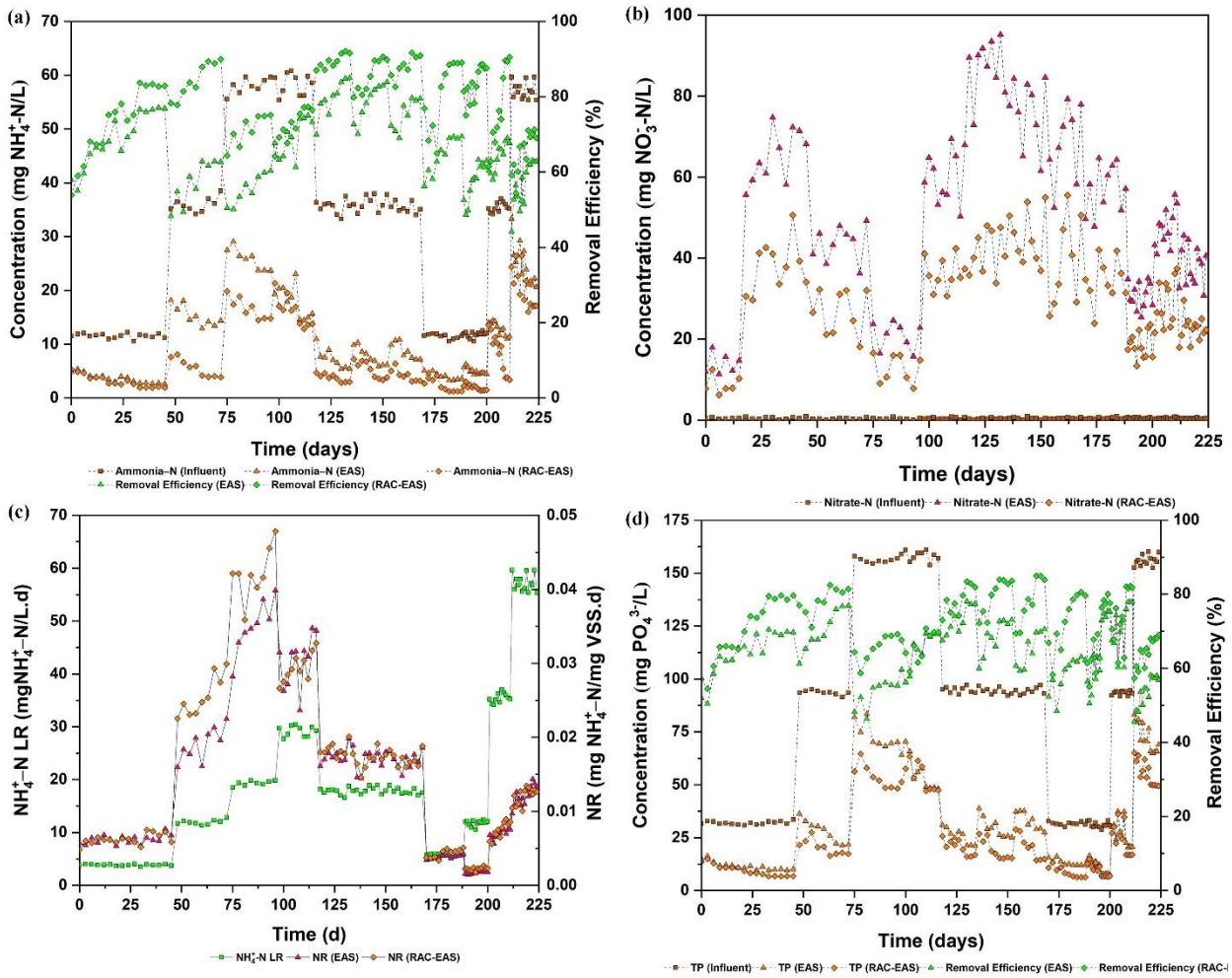

Fig. 2. The experimental time course of EAS and RAC-EAS bioreactors in terms of (a) NH_4^+-N concentrations and their removal efficiencies (b) influent and effluent nitrates (c) nitrification rate, (d) TP concentrations and their removal efficiencies

3.5. Bio-kinetic models for PPBE treatment in the EAS and RAC-EAS bioreactors

In bioreactor kinetic modelling, several good models were employed to generate kinetic assessments of various bioreactor accomplishments during wastewater treatment (Kutty et al., 2011). In this work, the performance of the EAS and RAC-EAS bioreactors were analyzed under various organics, nutrients, and hydraulic loadings. The results showed that, at high loading rates, extremely high nutrient removal efficiencies may be achieved. The entire kinetics of nutrient removal in bioreactors has been described using a variety of methodologies. To investigate Ammonia-N and TP removal in the bioreactors, three bio-kinetic models were

chosen. A graphical method was utilized to evaluate kinetic parameters based on Ammonia-N and TP, and the finest line was generated using the least squares linear regression algorithm. In the regression analysis, the mean steady-state values of the parameters measured during a period 2-3 times higher than the HRT were used (Rashtbari et al., 2022). Throughout the bioreactor experimentation phase, steady-state conditions persisted (Polat Bulut and Aslan, 2021).

3.5.1. First order model

The first-order kinetic model basically shows how adjustments in HRT affects system efficacy. In this study, the slope of the graph was determined by plotting the mean specific substrate removal rate against the mean effluent ammonia, which matched the bioreactor's nutrient removal bio-kinetics (k). Subsequently, $(S_{in} - S_{ef})$ /τ vs S_{ef} in Eq (S3) were plotted from the slope of the line at steady-state after computing the first-order bio-kinetic model coefficients k_1 and R^2. The plot of $(S_{in} - S_{ef})$ /τ and S_{ef} produced a linear line as portrayed in Fig. 3.

In EAS, constants for Ammonia-N removal were found to be 0.5936 and 0.2343, for k_1 and R^2 respectively, while the constants for TP removal were 0.5823 and 0.3176, respectively. Ammonia-N removal constants in RAC-EAS were found to be 1.1808 and 0.5902, for k_1 and R^2 respectively, while TP removal constants were 1.0229 and 0.5097, respectively. The poor R^2 values for both bioreactors indicate that the first-order model seems unable to predict Ammonia-N and TP removal efficiencies adequately. The k_1 value was low in first-order kinetics. The first-order model constant in this study was bigger than the value obtained by several researchers. Variations in k_1 levels may be caused by differences in operating circumstances and effluent kind (Pahlavanzadeh et al., 2018). The higher k_1 value indicated that the PPBE used as feed was so much more biodegradable. The nutrients kinetic yields the rate of Ammonia-N conversion to nitrate, which consequently indicates the rate of nitrifier growth. As a result, the findings from this research did not support this notion. This is in line with a study by (Kutty et al., 2011), who found k_1 and R^2 to be 1.2518 d^{-1} with a coefficient of 0.4872. On the other hand, a study by

(Faridnasr et al., 2016) found 33.533, 16.990, 13.988, and 7.891 as fixed values for concentrations of 0.5, 1.0, 1.5, and 2.5 g/L, respectively, and deduced that the scientific findings fit this model. Thus, the model conduct was amazing in terms of obtained correlation coefficients. This could be due in part to the several other operating parameters considered in the study.

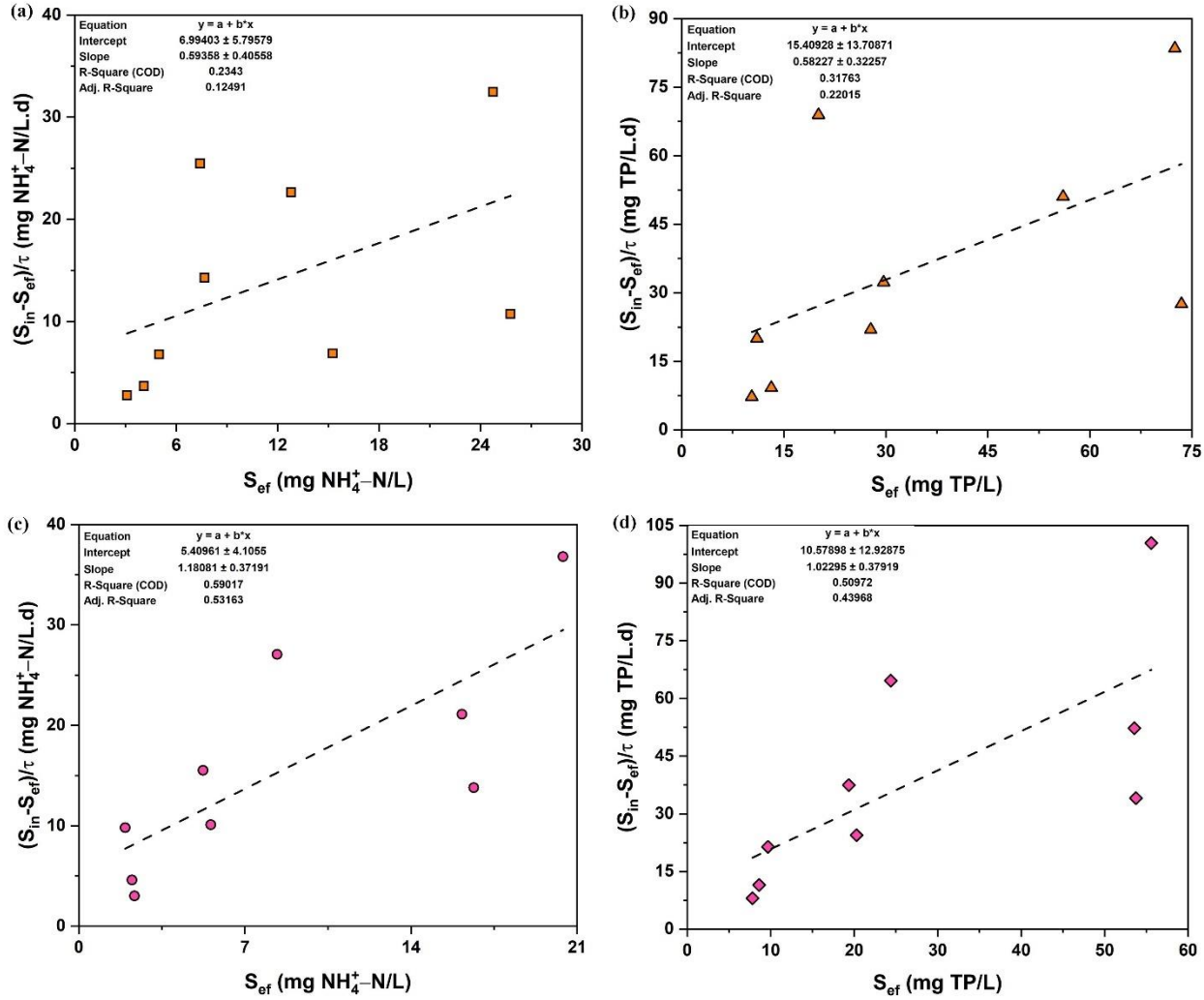

Fig. 3. First-order kinetic plot (a) Ammonia-N for EAS (b) TP for EAS (c) Ammonia-N for RAC-EAS and **(**d) TP for RAC-EAS

3.5.2. Grau second-order model

To derive the bio-kinetic coefficients, Eq. (S6) was shown in Fig. 4. The linear line's slope and intercept were utilized to compute n and m, respectively. The $_c$ and *d* values for Ammonia-N

removal in EAS, were 1.6106 and 0.8760, respectively. For TP removal, the corresponding values are 1.6091 and 0.9132, respectively. The *c* and *d* values for Ammonia-N removal in RAC-EAS were 1.2452 and 0.9595, respectively. For TP removal, the corresponding values were 1.3328 and 0.9586, respectively. The influent Ammonia-N and TP concentrations, and also the biomass concentration in the bioreactor, determine the k_S value. It increases when the effectiveness of substrate removal improves. The k_S values for Ammonia-N and TP in this investigation were 0.1188 per day and 0.8561 per day, respectively. A study by (Burman and Sinha, 2020) computed k_S values as 0.44, 0.57, 0.80, and 0.53 d^{-1} for attached growth, An-HMBR, suspended growth, and An-HBR system respectively, while (Faridnasr et al., 2016) in their study stated that the best correlation coefficient (R^2 = 0.9999) was obtained at 500 mg/L influent substrate concentration. The *c* and *d* values almost match those discovered in a study by (Polat Bulut and Aslan, 2021), where *c* and *d* were found to be 1.007 and 0.047, respectively. Interestingly, the *c*=0.033 and *d*=1.192 values published in another investigation by (Molaei et al., 2022)] were in agreement with the outputs reported by (Faridnasr et al., 2016). Nonetheless, the second-order kinetic, was not suitable for modelling the digestion process described in a study by (Nweke and Nwabanne, 2021). The substrate removal constant reported in a study authored by (Pahlavanzadeh et al., 2018) was well within the spectrum of *ks* values reported in earlier research for an influent TP phosphorus concentration of 235 mg/L at a HRT of 2 hours 30 minutes. The derived equation, which had a correlation coefficient of 0.98, confirmed that the model fit the existing results of the experiment.

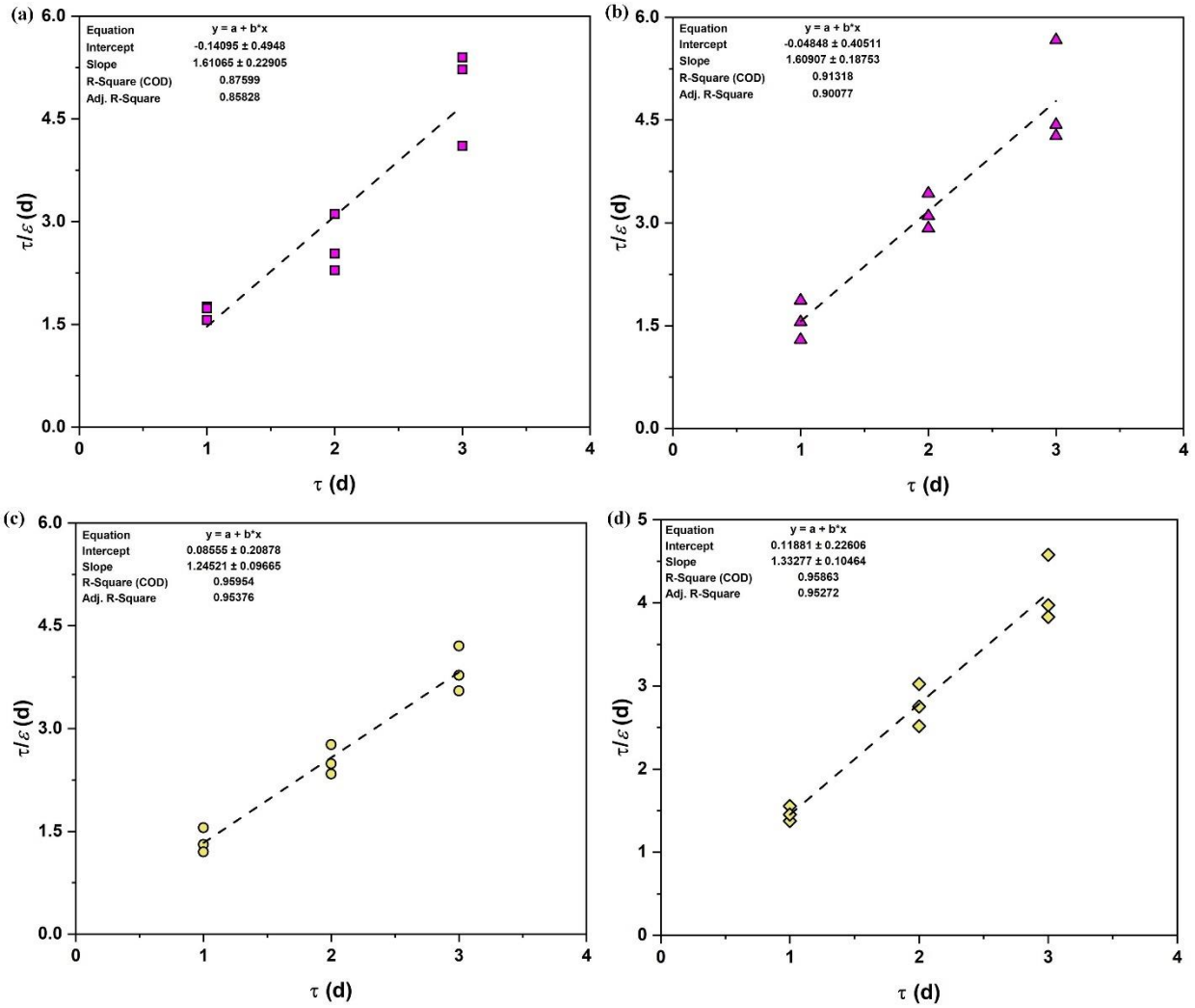

Fig. 4: Second-order kinetic plot (a) Ammonia-N for EAS (b) TP for EAS (c) Ammonia-N for RAC-EAS and (d) TP for RAC-EAS

3.5.3. Modified stover–kincannon model

The substrate consumption rate is much accurately understood as the nutrient loading rate by monomolecular kinetics in the modified stover model, commonly used in modeling biological reactors for wastewater treatment. Rather than using the surface reactor volume, the reactor volume is used. The model has been frequently utilized to find the bio-kinetic coefficients of a contact growth bioreactor system since it has a strong correlation compared to the other models. The model includes factors for estimating the efficacy and performance of a functioning biological system. The trickling filter was the first for the modified stover–kincannon model.

Most of the findings suggest that as the substrate concentration rises, so does the rate of substrate removal.

In this study, $\frac{v_R}{Q(S_{in}-S_{ef})}$ versus $\frac{v_R}{QS_{in}}$ was plotted to obtain the bio-kinetic coefficients (see Fig. 5). The coefficients are important in deciding a bioreactor's capacity for different types of wastewater and flow rates. The obtained coefficients can also be used to determine the bioreactor capacity needed to achieve the desired effluent substrate concentration (Pahlavanzadeh et al., 2018). For each concentration, the straight line in Fig. 5 depicts the association among Ammonia-N/TP loading rate and specific substrate utilization rate. The saturation value constant (K_v) and maximum utilization rate (U_{msr}) for Ammonia-N and TP removals were calculated using the line depicted on the graph.

In EAS, the K_v and U_{msr} values for Ammonia-N were 312.5 g/L.d and 348.66 g/L.d respectively, whereas those for TP removal were 909.1 g/L/d and 1132.1g/L/d. respectively. Whereas in RAC-EAS, the K_v and U_{msr} values for Ammonia-N were 532.1 g/L.d and 592.01 g/L.d respectively, and those for TP removal were 1227.0 g/L/d and 1407.2 g/L/d. respectively.The model's total loading approach has been found to be relevant to a variety of wastewaters. This includes domestic wastewater, slaughterhouse wastewater filters, pulp and paper wastewater, pickle wastewater and high-strength organic wastewater.

According to a study by (Bryant, 2010), the substrate removal plot for ammonia removal has $R^2 = 0.97$, with bio-kinetic coefficients like K_v and U_{msr} for ammonia being 0.477 and 1.27 g/L/d, respectively. The K_v was determined as 0.78, 32.54, 93.60, and 34.14, mg/L/d, and the maximum utilization rate (U_{msr}) was 0.36, 32.3, 45.5, and 33.8 mg/SS/d for attached growth, An-HMBR, suspended growth, and An-HBR system respectively (Burman and Sinha, 2020). An outstanding correlation coefficient R^2 of 0.9998 was recorded at an ammonia concentration of 200 mg/L. The values obtained for U_{msr} and K_v were 16.69 and 16.63 g/L.d, respectively. These U_{msr} and K_v values are < those observed in a study by (Nga et al., 2020), which suggested that the bioreactor had a huge potential for removing phosphorus. The impact of differing operational conditions

and bioreactor structures could be the cause of these contradicting results. A study by (Hooshyari et al., 2009) obtained U_{msr} and K_v values of 10.530– 13.960 g/L d and 9.2–10.5 g/L d, respectively, for an industrial wastewater with 30– 187 mg/L ammonia content. Irrespective of whether the bio-kinetic models are zero, first, or second order, the Stover–Kincannon model can predict Ammonia-N and TP decrease and treatment efficacy under every loading state. The Stover–Kincannon model also overlooks Ammonia-N and TP diffusion, along with hydraulic dynamics and other considerations (Chan et al., 2017; Jagaba et al., 2021b; Lee et al., 2017).

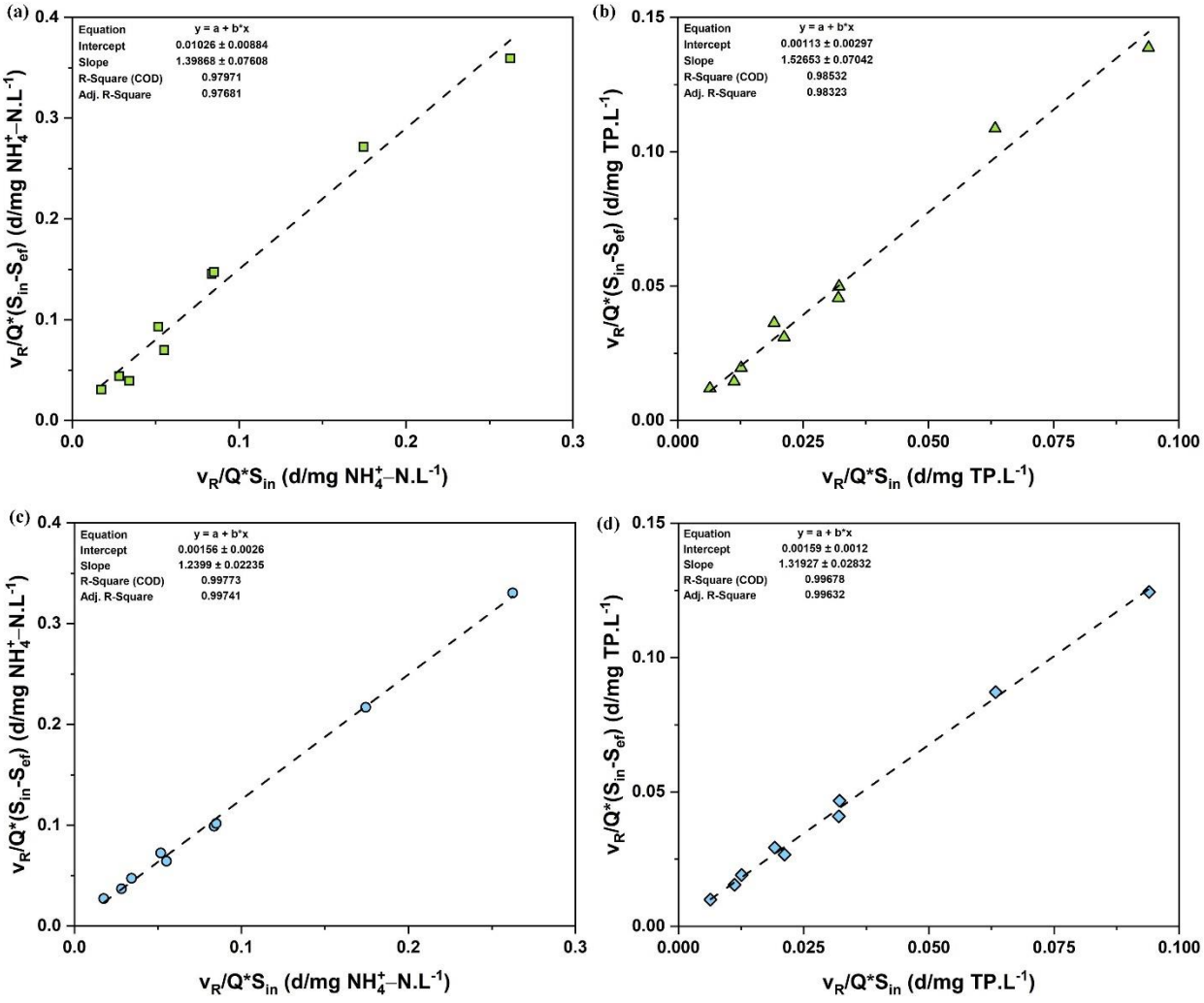

Fig. 5: Modified stover kinetic plot (a) Ammonia-N for EAS (b) TP for EAS (c) Ammonia-N for RAC-EAS and **(**d) TP for RAC-EAS

4. Conclusion

This study evaluates the effectiveness of the EAS and RAC-EAS for the treatment of PPBE by employing RAC. The efficiency of the treatment technique was determined by the amount of nutrients removed with associated MLSS and MLVSS. Findings revealed that:

- 84.51% and 77.62% highest reduction in Ammonia-N and TP were recorded respectively for the EAS. Interestingly, the RAC-EAS recorded higher removal efficiency of 91.71% and 84.64% for Ammonia-N and TP respectively. NH_4^+-N and NO_2^--N values were below the industrial discharges limit. Lesser nitrite/nitrate levels, higher TP removal, and TP removal via increased biological TP removal were all evidence of superior nitrogen and TP removal in RAC-EAS.
- During the RSM optimization, the specified and response models for p-values less than 5%, were found to be significant, as were quadratic models. The maximum nutrient removal efficiencies were attained at 2-day HRT and 60% PPBE concentration.
- In EAS, high correlation coefficients R^2 of 0.9797 and 0.9853 were recorded in the Modified Stover–Kincannon model for Ammonia-N and TP, respectively. The RAC-EAS had 0.9977 and 0.9968 for Ammonia-N and TP respectively. The modified Stover-Kincannon and Grau second-order models tend to be the best at describing the bio-kinetic activity in the EAS and RAC-EAS bioreactors that best suit the data sets. As a result, the models can also be used to develop EAS and RAC-EAS bioreactors, as well as anticipate their behaviour. However, the further evaluation of the removal by-products needs to be studied for possible recontamination and viability of the process at field scale for adoption is necessary for sustainable and safe industrial wastewater disposal.

Acknowledgement

The authors would like to express their gratitude to Universiti Teknologi PETRONAS (UTP) for supporting the research. The authors are also grateful to the Researchers Supporting Project number (RSP-2021/8), King Saud University, Riyadh, Saudi Arabia for the financial support.

References

Abubakar, S., et al., 2016. Quality water analysis of public and private boreholes (a case study of Azare Town, Bauchi, Nigeria). Am J Eng Res. 5, 204-8.

Adel, S., et al., 2020. Evaluation the performance of sequencing batch reactor and bio-film sequencing batch reactor for pulp and paper wastewater treatment. Desalination and water treatment 208, 136-147.

Ahmed, D. N., et al., 2020. Waste foundry sand/MgFe-layered double hydroxides composite material for efficient removal of Congo red dye from aqueous solution. Scientific Reports. 10, 1-12.

Al-mahbashi, N., et al., 2022. Column Study for Adsorption of Copper and Cadmium Using Activated Carbon Derived from Sewage Sludge. Advances in Civil Engineering.

Al-Rekabi, W. S., et al., 2017. Municipal wastewater treatment of basrah city using intermittent cycle extended aeration system (ICEAS). Journal of Engineering and Sustainable Development. 21, 1-14.

Alhassan, M., et al., 2018. Comparative studies of CO_2 capture using acid and base modified activated carbon from sugarcane bagasse. Biofuels. 9, 719-728.

Ali, M., Sreekrishnan, T., 2001. Aquatic toxicity from pulp and paper mill effluents: a review. Advances in environmental research. 5, 175-196.

Asfaram, A., et al., 2015. Removal of basic dye Auramine-O by ZnS: Cu nanoparticles loaded on activated carbon: optimization of parameters using response surface methodology with central composite design. RSC advances. 5, 18438-18450.

Assadi, A., et al., 2018. Anaerobic–aerobic sequencing batch reactor treating azo dye containing wastewater: effect of high nitrate ions and salt. Journal of Water Reuse and Desalination. 8, 251-261.

Ayaz, S. C., et al., 2012. Phosphorus removal and effect of adsorbent type in a constructed wetland system. Desalination and water treatment. 37, 152-159.

Azmi, N. B., et al., 2016. Anaerobic stabilized landfill leachate treatment using chemically activated sugarcane bagasse activated carbon: kinetic and equilibrium study. Desalination and Water Treatment. 57, 3916-3927.

Bawiec, A., 2019. Efficiency of nitrogen and phosphorus compounds removal in hydroponic wastewater treatment plant. Environmental Technology. 40, 2062-2072.

Birniwa, A. H., et al., 2021. Polypyrrole-polyethyleneimine (PPy-PEI) nanocomposite: An effective adsorbent for nickel ion adsorption from aqueous solution. Journal of Macromolecular Science, Part A. 58, 206-217.

Borba, V., et al., 2021. New data on eggshell structure of capillariid species: A SEM perspective. Parasitology Research. 120, 963-970.

Bryant, C. W., 2010. Updating a model of pulp and paper wastewater treatment in a partial-mix aerated stabilization basin system. Water Science and Technology. 62, 1248-1255.

Burman, I., Sinha, A., 2020. Performance evaluation and substrate removal kinetics in an up-flow anaerobic hybrid membrane bioreactor treating simulated high-strength wastewater. Environmental Technology. 41, 309-321.

Cai, F., et al., 2019. Different bioreactors for treating secondary effluent from recycled paper mill. Science of The Total Environment. 667, 49-56.

Chan, Y. J., et al., 2017. Performance and kinetic evaluation of an integrated anaerobic–aerobic bioreactor in the treatment of palm oil mill effluent. Environmental technology. 38, 1005-1021.

Dan, N. H., et al., 2020. Removal of nutrients from anaerobically digested swine wastewater using an intermittent cycle extended aeration system. Frontiers in microbiology. 2515.

de Palma, K. R., et al., 2021. The influence of the elemental and structural chemical composition on the ash fusibility of sugarcane bagasse and sugarcane straw. Fuel. 304, 121404.

Faizal, M., The Effect of Retention Time and Initial Concentration of Ammonia on Biological Treatment for Reducing Ammonia Content in Wastewater. Sriwijaya International Seminar on Energy-Environmental Science and Technology, Vol. 1, 2014, 186-190.

Faridnasr, M., et al., 2016. Optimization of the moving-bed biofilm sequencing batch reactor (MBSBR) to control aeration time by kinetic computational modeling: simulated sugar-industry wastewater treatment. Bioresource technology. 208, 149-160.

Farooqi, I., Basheer, F., 2017. Treatment of Adsorbable Organic Halide (AOX) from pulp and paper industry wastewater using aerobic granules in pilot scale SBR. Journal of Water Process Engineering. 19, 60-66.

Hooshyari, B., et al., 2009. Kinetic analysis of enhanced biological phosphorus removal in a hybrid integrated fixed film activated sludge process. International Journal of Environmental Science & Technology. 6, 149-158.

Imran, M., Khan, A. A., 2018. Characterization of agricultural waste sugarcane bagasse ash at 1100 C with various hours. Materials Today: Proceedings. 5, 3346-3352.

Jaafarzadeh, N., et al., 2010. Evaluation of biological landfill leachate treatment incorporating struvite precipitation and powdered activated carbon addition. Waste management & research. 28, 759-766.

Jagaba, A. H., et al., 2019. Defluoridation of drinking water by activated carbon prepared from tridax procumbens plant (A Case Study of Gashaka Village, Hong LGA, Adamawa State, Nigeria). International Journal of Computational Theoretical Chemistry. 7, 1.

Jagaba, A. H., et al., Effect of Hydraulic Retention Time on the Treatment of Pulp and Paper Industry Wastewater by Extended Aeration Activated Sludge System. 2021 Third International Sustainability and Resilience Conference: Climate Change. IEEE, 2021a, 221-224.

Jagaba, A. H., et al., Effect of Environmental and Operational Parameters on Sequential Batch Reactor Systems in Dye Degradation. Dye Biodegradation, Mechanisms and Techniques. Springer, 2022a, 193-225.

Jagaba, A. H., et al., 2022b. Diverse sustainable materials for the treatment of petroleum sludge and remediation of contaminated sites: a review. Cleaner Waste Systems. 100010.

Jagaba, A. H., et al., 2022c. Parametric optimization and kinetic modelling for organic matter removal from agro-waste derived paper packaging biorefinery wastewater. Biomass Conversion and Biorefinery. 1-18.

Jagaba, A. H., et al., 2021b. A systematic literature review of biocarriers: Central elements for biofilm formation, organic and nutrients removal in sequencing batch biofilm reactor. Journal of Water Process Engineering. 42, 102178.

Jagaba, A. H., et al., 2022d. Kinetics of Pulp and Paper Wastewater Treatment by High Sludge Retention Time Activated Sludge Process. Journal of Hunan University Natural Sciences. 49.

Jin, P., et al., 2013. Biological activated carbon treatment process for advanced water and wastewater treatment. Biomass Now-Cultivation and Utilization. 153-192.

Kalkan, Ç., et al., 2011. Evaluation of biological activated carbon (BAC) process in wastewater treatment secondary effluent for reclamation purposes. Desalination. 265, 266-273.

Korotta-Gamage, S. M., Sathasivan, A., 2017. A review: Potential and challenges of biologically activated carbon to remove natural organic matter in drinking water purification process. Chemosphere. 167, 120-138.

Koupaie, E. H., et al., 2013. Evaluation of integrated anaerobic/aerobic fixed-bed sequencing batch biofilm reactor for decolorization and biodegradation of azo dye Acid Red 18: Comparison of using two types of packing media. Bioresource technology. 127, 415-421.

Kutty, S., et al., 2011. The Effects of Ammonia Loading on the Nitrification Kinetics of Aerobic Baffled Continuous Biological Reactor. Procedia Environmental Sciences. 10, 1350-1356.

Lawal, I. M., et al., 2021. Multi-Criteria Performance Evaluation of Gridded Precipitation and Temperature Products in Data-Sparse Regions. Atmosphere. 12, 1597.

Lee, C.-G., et al., 2017. Removal of copper, nickel and chromium mixtures from metal plating wastewater by adsorption with modified carbon foam. Chemosphere. 166, 203-211.

Liang, J., et al., 2021. Performance and microbial communities of a novel integrated industrial-scale pulp and paper wastewater treatment plant. Journal of Cleaner Production. 278, 123896.

Lo, C., et al., 1994. Enhanced nutrient removal by oxidation-reduction potential (ORP) controlled aeration in a laboratory scale extended aeration treatment system. Water Research. 28, 2087-2094.

Maged, A., et al., 2021. New mechanistic insight into rapid adsorption of pharmaceuticals from water utilizing activated biochar. Environmental Research. 202, 111693.

Mareai, B. M., et al., 2020. Performance comparison of phenol removal in pharmaceutical wastewater by activated sludge and extended aeration augmented with activated carbon. Alexandria Engineering Journal. 59, 5187-5196.

Mo, J., et al., 2018. A review on agro-industrial waste (AIW) derived adsorbents for water and wastewater treatment. Journal of environmental management. 227, 395-405.

Mohammadi, N., et al., 2011. Adsorption process of methyl orange dye onto mesoporous carbon material–kinetic and thermodynamic studies. Journal of colloid and interface science. 362, 457-462.

Molaei, S., et al., 2022. Biodegradation of the petroleum hydrocarbons using an anoxic packed-bed biofilm reactor with in-situ biosurfactant-producing bacteria. Journal of Hazardous Materials. 421, 126699.

Nam, H., et al., 2018. Development of rice straw activated carbon and its utilizations. Journal of environmental chemical engineering. 6, 5221-5229.

Nandiyanto, A. B. D., et al., 2017. Porous activated carbon particles from rice straw waste and their adsorption properties. Journal of Engineering Science and Technology. 12, 1-11.

Nasara, M. A., et al., 2021. Assessment of Non-Revenue Water Management Practices in Nigeria (A Case Study of Bauchi State Water and Sewerage Cooperation). American Journal of Engineering Research. 10, 390-401.

Nath, K., Bhakhar, M. S., 2011. Microbial regeneration of spent activated carbon dispersed with organic contaminants: mechanism, efficiency, and kinetic models. Environmental Science and Pollution Research. 18, 534-546.

Naushad, M., 2014. Surfactant assisted nano-composite cation exchanger: development, characterization and applications for the removal of toxic Pb2+ from aqueous medium. Chemical Engineering Journal. 235, 100-108.

Naushad, M., et al., 2019. Adsorption kinetics, isotherm and reusability studies for the removal of cationic dye from aqueous medium using arginine modified activated carbon. Journal of Molecular Liquids. 293, 111442.

Ng, J., et al., Organic and nutrient removal for domestic wastewater treatment using bench-scale sequencing batch reactor. AIP Conference Proceedings, Vol. 2339. AIP Publishing LLC, 2021, 020139.

Nga, D. T., et al., 2020. Kinetic modeling of organic and nitrogen removal from domestic wastewater in a down-flow hanging sponge bioreactor. Environmental Engineering Research. 25, 243-250.

Noor, A., et al., Bio-kinetics of organic removal in EAAS reactor for co-treatment of refinery wastewater with municipal wastewater. IOP Conference Series: Materials Science and Engineering, Vol. 1092. IOP Publishing, 2021a, 012068.

Noor, A., et al., Kinetic modelling of nutrient removal of petroleum industry wastewater remediation. 2021 Third International Sustainability and Resilience Conference: Climate Change. IEEE, 2021b, 216-220.

Nweke, C. N., Nwabanne, J. T., 2021. Anaerobic Digestion of Yam Peel for Biogas Production: A Kinetic Study. Journal of Engineering and Applied Sciences. 18, 275-286.

Pahlavanzadeh, S., et al., 2018. Performance and kinetic modeling of an aerated submerged fixed-film bioreactor for BOD and nitrogen removal from municipal wastewater. Journal of environmental chemical engineering. 6, 6154-6164.

Pereira, P., et al., 2014. Sugarcane bagasse cellulose fibres and their hydrous niobium phosphate composites: synthesis and characterization by XPS, XRD and SEM. Cellulose. 21, 641-652.

Polat Bulut, A., Aslan, Ş., 2021. A kinetic study on the nitrification process in the upflow submerged biofilter reactor. Environmental Technology. 1-9.

Rasheed, T., et al., 2020. Surfactants-based remediation as an effective approach for removal of environmental pollutants—A review. Journal of Molecular Liquids. 318, 113960.

Rashtbari, Y., et al., 2022. Green synthesis of zero-valent iron nanoparticles and loading effect on activated carbon for furfural adsorption. Chemosphere. 287, 132114.

Rosales-Calderon, O., Arantes, V., 2019. A review on commercial-scale high-value products that can be produced alongside cellulosic ethanol. Biotechnology for biofuels. 12, 1-58.

Saeed, A. A. H., et al., 2021. Modeling and optimization of biochar based adsorbent derived from Kenaf using response surface methodology on adsorption of Cd^{2+}. Water. 13, 999.

Sarkar, S., et al., 2020. Investigations on porous carbon derived from sugarcane bagasse as an electrode material for supercapacitors. Biomass and Bioenergy. 142, 105730.

Sarvajith, M., Nancharaiah, Y., 2022. Enhancing biological nitrogen and phosphorus removal performance in aerobic granular sludge sequencing batch reactors by activated carbon particles. Journal of environmental management. 303, 114134.

Shitu, A., et al., 2020. Performance of novel sponge biocarrier in MBBR treating recirculating aquaculture systems wastewater: Microbial community and kinetic study. Journal of Environmental Management. 275, 111264.

Stewart, F. M., et al., 2008. Floating islands as an alternative to constructed wetlands for treatment of excess nutrients from agricultural and municipal wastes–results of laboratory-scale tests. Land Contamination & Reclamation. 16, 25-33.

Tahir, H., et al., 2016. Application of natural and modified sugar cane bagasse for the removal of dye from aqueous solution. Journal of Saudi Chemical Society. 20, S115-S121.

Toczyłowska-Mamińska, R., 2017. Limits and perspectives of pulp and paper industry wastewater treatment–A review. Renewable and Sustainable Energy Reviews. 78, 764-772.

Tsang, Y. F., et al., 2006. A novel technology for bulking control in biological wastewater treatment plant for pulp and paper making industry. Biochemical Engineering Journal. 32, 127-134.

Tummino, M. L., et al., 2019. Green waste-derived substances immobilized on SBA-15 silica: Surface properties, adsorbing and photosensitizing activities towards organic and inorganic substrates. Nanomaterials. 9, 162.

Umar, H., et al., 2021. Assessing the implementation levels of oil palm waste conversion methods in Malaysia and the challenges of commercialisation: Towards sustainable energy production. Biomass and Bioenergy. 151, 106179.

Wagemann, K., Tippkötter, N., 2018. Biorefineries: a short introduction. Biorefineries. 1-11.

Wang, D., et al., 2016. Evaluating the removal of organic fraction of commingled chemical industrial wastewater by activated sludge process augmented with powdered activated carbon. Arabian Journal of Chemistry. 9, S1951-S1961.

Xiao, G., et al., 2019. Superior adsorption performance of graphitic carbon nitride nanosheets for both cationic and anionic heavy metals from wastewater. Chinese Journal of Chemical Engineering. 27, 305-313.

Yu, L., et al., 2015. Microbial community structure associated with treatment of azo dye in a start-up anaerobic sequenced batch reactor. Journal of the Taiwan Institute of Chemical Engineers. 54, 118-124.

Zhang, X., et al., 2017. Behavior of nitrogen removal in an aerobic sponge based moving bed biofilm reactor. Bioresource technology. 245, 1282-1285.

Zhou, G., et al., 2018. Efficient heavy metal removal from industrial melting effluent using fixed-bed process based on porous hydrogel adsorbents. Water research. 131, 246-254.